On Multiplexing Models for Independent Traffic Flows in Single- and Multi-Node Networks

Amr Rizk, *Student Member, IEEE,* and Markus Fidler, *Senior Member, IEEE*

***Abstract*—In packet switched networks, statistical multiplexing of independent variable bit rate flows achieves significant resource savings, i.e., N flows require considerably less than N times the resources needed for one flow. In this work, we explore statistical multiplexing using methods from the current stochastic network calculus, where we compare the accuracy of different analytical approaches. While these approaches are known to provide identical results for a single flow, we find significant differences if several independent flows are multiplexed. Recent results on the concatenation of nodes along a network path allow us to investigate both single- as well as multi-node networks with cross traffic. The analysis enables us to distinguish different independence assumptions between traffic flows at a single node as well as between cross traffic flows at consecutive nodes of a network path. We contribute insights into the scaling of end-to-end delay bounds in the number of nodes n of a network path under statistical independence. Our work is complemented by numerical applications, e.g., on access multiplexer dimensioning and traffic trunk management.**

***Index Terms*—Statistical network calculus, statistical multiplexing, effective bandwidth, EBB.**

I. Introduction

RESOURCE sharing in today's communication networks potentiates significant statistical multiplexing gain. Prominent examples include Erlang's formulas for dimensioning of telecommunication systems as well as Kleinrock's proof of the efficiency of packet switching over circuit switching [2]. Multiplexing effects influence resource allocation schemes such as sharing a single buffered link by multiple data flows or multiple access schemes in wireless networks. A quantitative treatment of statistical multiplexing supports network dimensioning to ensure a certain quality of service (QoS). An example on the amount of resources needed to maintain a certain level of QoS can be used to illustrate the gain of statistical multiplexing. Assume a single traffic flow requires an amount of resources x to achieve a certain QoS. Given N independent traffic flows are multiplexed, the resource requirement for the aggregate to maintain the same level of QoS can be significantly smaller than $N \cdot x$ [3].

An important application is, e.g., the dimensioning of links and buffers at a DSL access multiplexer, where in uplink a large number of access links are multiplexed to a single backbone link. Typically, the aggregated capacity of the access links exceeds the capacity of the backbone link. This overbooking becomes feasible due to statistical multiplexing. The amount of overbooking has, however, implications on the QoS that is perceived by the customers, e.g., in terms of throughput, delay, and packet loss. Thus, it is vital to provide methods to evaluate the statistical multiplexing gain provided by the independence of the customers' traffic.

Moreover, we elaborate on statistical gain that can be exploited in the multi-node case. Consider a service provider deploying an MPLS traffic trunk over a path of n consecutive nodes. At the individual nodes, the trunk shares resources with other, so-called cross traffic flows. Considering the statistical multiplexing gain between these flows can conserve significant amounts of resources when dimensioning the traffic trunk. In particular, in this work we analyze the impact of statistical independence of cross traffic flows on the end-to-end performance of an n node path. The results can be used to formulate traffic and service contracts, or given a target QoS, they can be applied for network resource management, e.g., to perform admission control.

The analysis of statistical multiplexing has been of great interest already in ATM networks, see the seminal work [4]. In the context of multiplexing, numerous works analyze performance criteria such as the mean or percentile of the backlog or delay distributions. This allows, for example, buffer dimensioning with respect to these target criteria. It also permits the calculation of the number of admissible flows under a target QoS constraint, [5]–[9]. The evaluation of such target criteria for multiplexed independent traffic is treated using various mathematical models which include queueing theory, the theory of effective bandwidths, and the stochastic network calculus. We use the stochastic network calculus that enables us to investigate additional statistical effects that are specific to scheduling as well as multi-node networks.

In this work, we seek to answer questions on network performance management and service provisioning under the aspect of statistical multiplexing. To this end, we employ the stochastic network calculus to examine multiplexing effects. The framework of the stochastic network calculus enables the derivation of statistical end-to-end bounds on performance metrics, such as backlog and delay, for networks under various types of traffic. We introduce the needed background on statistical traffic description, i.e., different, commonly used traffic envelopes [10]–[16]. We contrast respective methods for the derivation of performance bounds from these envelopes and provide a comparison of their accuracy. We review how

Manuscript received February 3, 2012; revised July 26, 2012. The associate editors coordinating the review of this paper and approving it for publication were P. Sinha, J. Xu, and B. Lin (corresponding guest editors).

This work was supported by an Emmy Noether grant from the German Research Foundation (DFG). Parts of this work have been presented in the earlier paper [1] at IEEE/ACM IWQoS'11.

The authors are with the Institute of Communications Technology, Leibniz Universität Hannover, Germany (e-mail: {amr.rizk, markus.fidler}@ikt.uni-hannover.de).

Digital Object Identifier 10.1109/TNSM.2012.091012.120234

these methods are related, such that they yield the same performance bounds for a single flow. In contrast, in case of multiplexing several flows we find that the methods differ regarding the obtained performance bounds. We provide analytical justifications for these differences and show a comprehensive numerical comparison. Our results highlight the importance of considering statistical independence using appropriate methods. Further we analyze tandem networks with end-to-end through flows, that share resources at individual nodes with multiplexed cross flows. We show statistical multiplexing effects between independent cross traffic flows at tandem queues on end-to-end delay bounds for the through flows. We contribute a scaling of end-to-end performance bounds with increasing network path length under statistical independence. Finally we compare the findings to existing scaling results that stem from different models.

The remainder of this paper is structured as follows. In Sect. II we review statistical models of packet data traffic known from literature and introduce needed definitions. Next, in Sect. III we provide an analysis of traffic models under multiplexing in the context of the stochastic network calculus. In Sect. IV we review stochastic service models as known from the literature and exemplify the benefit of scheduling in conjunction with statistical multiplexing. In Sect. V we present multiplexing gain in so called convolution-form networks [17], where we derive a scaling of end-to-end delay bounds under independent cross traffic. We summarize the conclusions in Sect. VI.

II. Statistical Envelope Models

In this section, we review statistical models for characterizing packet data traffic as known from the literature, see [10]–[16], [18] as well as [19] for a survey. We use the concept of envelopes that are statistical bounds on the amount of traffic arrivals that are violated at most by a certain probability. We review the construction and relation of different types of envelopes known from the literature and show how performance bounds at a single node can be computed using respective methods. In addition to the construction of arbitrarily shaped envelopes we inspect envelopes of a special shape, i.e., affine envelopes, which we use throughout the remainder of the paper. We present corresponding performance bounds and review their relation to the affine shape of the envelopes.

A. Definition and Construction of Envelopes

The concept of arrival envelopes dates back to the seminal work of Cruz [20] and is used in conjunction with the notion of service curves [21] to derive performance bounds for data networks. In the context of stochastic network calculus the derived bounds, e.g., on backlog or delay, are allowed to be violated by a certain (small) probability.

In this work we consider discrete time traffic arrivals, that are given by the doubly indexed term $A(\tau,t)$ which denotes the amount of traffic that arrived in the time interval $[\tau,t)$, where $\tau,t \in \mathbb{N}_0$. We write $A(t)$ for $A(0,t)$ whenever possible for convenience, with $A(0)=0$ by definition. We assume that the arrivals are stationary such that $\mathsf{P}[A(0,t)\geq x] = \mathsf{P}[A(\tau,\tau+t)\geq x]$ holds for all τ, t, and $x \geq 0$.

We use moment generating functions (MGF) given by

$$\mathsf{M}_X(\theta,t) = \mathsf{E}\left[e^{\theta X(\tau,\tau+t)}\right]$$

with parameter $\theta \in \mathbb{R}$ to characterize stationary random processes $X(\tau,\tau+t)$ for any $t\geq 0$. Given the MGF, envelopes are frequently constructed by invoking Chernoff's theorem

$$\mathsf{P}[X(\tau,\tau+t)\geq x] \leq e^{-\theta x}\mathsf{M}_X(\theta,t)$$

where $\theta \geq 0$ is a free parameter that can be optimized to minimize the right hand side. Note that due to the inequality above, one can conveniently substitute the MGF $\mathsf{M}_X(\theta,t)$ by an upper bound (for all $\theta\geq 0$ and $t \geq 0$) if the exact MGF is not known. There exist bounds on the MGF for many types of traffic $A(\tau,t)$, such as Markovian, regulated, or self-similar traffic [5].

Next, we consider statistical envelopes E with parameter $b\geq 0$ that are defined in [14] as

$$\mathsf{P}[A(\tau,t) - E(t-\tau) > b] \leq \varepsilon^p(b). \tag{1}$$

The definition formalizes the probability that the arrivals $A(\tau,t)$ exceed the envelope $E(t-\tau)$ by more than b. The superscript p refers to the probability of envelope violation by *any* traffic realization at *one* point in time. The construction of such envelopes can be carried out by invoking Chernoff's theorem, e.g., [22], such that

$$\mathsf{P}[A(\tau,t) - E(t-\tau) > b] \leq e^{-\theta b}\mathsf{M}_{A-E}(\theta,t-\tau) \tag{2}$$

where the right hand side is a solution for $\varepsilon^p(b)$ from (1). Note that $\varepsilon^p(b)$ decays exponentially fast with parameter b. The MGF $\mathsf{M}_{A-E}(\theta,t-\tau)$ is obtained as

$$\begin{aligned}\mathsf{M}_{A-E}(\theta,t-\tau) &= \mathsf{E}\left[e^{\theta(A(\tau,t)-E(t-\tau))}\right]\\ &= \mathsf{M}_A(\theta,t-\tau)e^{-\theta E(t-\tau)}\end{aligned} \tag{3}$$

by the fact that $E(t-\tau)$ is a deterministic function. By insertion of (3) in (2) the violation probability $\varepsilon^p(b)$ follows.

For the derivation of performance bounds it is required that envelopes make guarantees for entire sample paths. This can be expressed similar to [11] and [14] as

$$\mathsf{P}\left[\sup_{\tau\in[0,t-1]}\{A(\tau,t)-E(t-\tau)\} > b\right] \leq \varepsilon^s(b) \tag{4}$$

where we use superscript s to refer to the probability of envelope violation at *any* point in time, i.e., anywhere along the sample path. By choice of $E(0)=0$ and since $A(t,t)=0$ by definition the term at $\tau=t$ is trivially zero. Hence, it is omitted from the supremum. We define the shorthand operator $\oslash$ as

$$A\oslash E(t) := \sup_{\tau\in[0,t-1]}\{A(\tau,t)-E(t-\tau)\}\,.$$

Invoking Chernoff's theorem for (4) yields

$$\mathsf{P}[A\oslash E(t) > b] \leq e^{-\theta b}\mathsf{M}_{A\oslash E}(\theta,t) \tag{5}$$

where the right hand side is a solution for $\varepsilon^s(b)$ from (4). A rigorous upper bound for the MGF $\mathsf{M}_{A\oslash E}(\theta,t)$ can be found using the union bound similarly as, e.g., in [11], [14] as

$$\mathsf{M}_{A\oslash E}(\theta,t) = \mathsf{E}\left[e^{\theta\left(\sup_{\tau\in[0,t-1]}\{A(\tau,t)-E(t-\tau)\}\right)}\right] \leq \sum_{\tau=0}^{t-1}\mathsf{E}\left[e^{\theta A(\tau,t)-E(t-\tau)}\right]. \quad (6)$$

The sample path violation probability $\varepsilon^s(b)$ from (4) is obtained with help of Chernoff's theorem in (5) and the evaluation of (6).

In Fig. 1 we provide a guided construction of traffic envelopes. Fig. 1 summarizes the logic sequence of (1)-(3) and (4)-(6).

We start from traffic arrivals $A(\tau,t)$ located at the top of Fig. 1. For many cases bounds on the MGF of $A(\tau,t)$ are known such that we typically begin with (3) at the point marked A1. With help of Chernoff's theorem we move from the left side to the right side of Fig 1. From point A1, i.e., a known bound on $\mathsf{M}_{A-E}(\theta,t-\tau)$, we move using Chernoff's theorem (2) to point B1. Point B1 marks the calculation of the violation probability $\varepsilon^p(b)$ as in (1).

If a statistical bound on the complementary cumulative distribution function (CCDF) of the arrivals exists, it is possible to move directly from $A(\tau,t)$ at the top of Fig. 1, down the dashed arrow to point B1.

Invoking the union bound induces a movement downwards in Fig. 1, thus replacing the point-wise treatment by a sample path analysis. Starting again from point A1, we can invoke the union bound and find a bound on $\mathsf{M}_{A\oslash E}$, i.e., (6), which is located at point A2. With help of Chernoff's theorem, i.e., (5) we move rightwards to point B2. Point B2 marks the sample path violation probability $\varepsilon^s(b)$ from (4).

Alternatively, the union bound can be applied to move downwards from point B1 to point B2 to find, e.g., [14],

$$\mathsf{P}[A\oslash E(t) > b] \leq \sum_{\tau=0}^{t-1}\mathsf{P}[A(\tau,t)-E(t-\tau) > b]. \quad (7)$$

The sample path violation probability $\varepsilon^s(b)$ from (4) is in this case obtained by evaluating the sum on the right hand side of (7), i.e., by summing $\varepsilon^p(b)$.

Note that the order of applying the union bound and Chernoff's theorem does not matter for the derivation of $\varepsilon^s(b)$ here. Indeed, when moving in Fig. 1 from point A1 to point B2 it is irrelevant with respect to the result, whether the intermediate step is point A2 or point B1. This is verified by comparing the right hand side of (5) to the right hand side of (7). Plugging (6) into (5) yields the same bound for $\varepsilon^s(b)$ as plugging (2) and the first line of (3) into (7).

The resulting sample path envelope (4) at point B2 is essential for the derivation of statistical performance bounds with a defined violation probability. To see the direct equivalence consider for example the backlog $B(t)$ at a constant rate server with capacity C, which can be written as

$$\mathsf{P}[B(t) > b] = \mathsf{P}[A\oslash C(t) > b] \quad (8)$$

using Lindley's equation [23]. This can be seen as a special case of (4) such that inserting $E(\tau)=C\tau$ into (4) leads to the backlog bound $\mathsf{P}[B(t)>b] \leq \varepsilon^s(b)$. Analogously, a FIFO delay bound W is found as $\mathsf{P}[W(t) > b/C] \leq \varepsilon^s(b)$ with identical violation probability $\varepsilon^s(b)$.

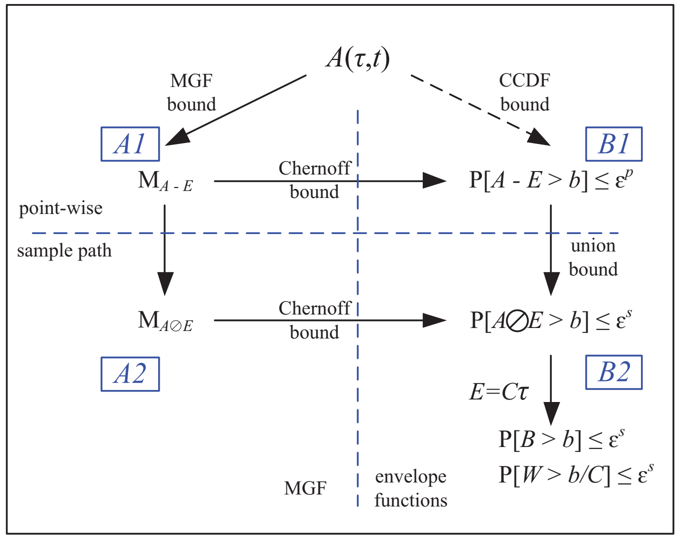

Fig. 1. Construction of envelopes $E(t)$ with violation probability ε. Depicted left are MGFs (A1, A2) and right are envelopes (B1, B2). Chernoff's bound allows deriving envelopes from the MGF of arrivals. Point-wise arguments are in the top (A1, B1) and sample path arguments in the bottom (A2, B2). Sample path arguments follow by use of the union bound and yield bounds for the backlog B and delay W if $C\tau$ is substituted for $E(\tau)$.

In this section we reviewed the basic steps needed for the derivation of sample path envelopes starting from a bound on the MGF of the traffic arrivals. We can find the desired envelopes and subsequent performance bounds using a navigation through Fig. 1. Next, we will show how respective computations are performed for the important class of exponentially bounded traffic.

B. Affine Envelopes and Exponentially Bounded Burstiness

Since the work of Cruz [20] affine envelopes, i.e., envelopes of the type $b+rt$, attracted considerable attention. These envelopes are especially elegant in the derivation of performance bounds, e.g, for backlog and delay, at a work-conserving constant rate server. For instance, for a server with capacity C, the parameter b is a backlog bound as long as the envelope rate $r<C$. In the sequel we demonstrate examples of performance bounds derived for affine envelopes.

In [12], [23] Chang devises a stochastic $(\sigma(\theta),\rho(\theta))$ traffic model. The $(\sigma(\theta),\rho(\theta))$ model defines the affine MGF bound

$$\mathsf{M}_A(\theta,\tau) \leq e^{\theta(\sigma(\theta)+\rho(\theta)\tau)} \quad (9)$$

for $\theta\geq 0$ and $\tau\geq 0$. The envelope rate $\rho(\theta)$ is closely related to the notion of effective bandwidths [5], [23]. To transition from point A1 to A2 in Fig. 1, we insert the MGF bound (9) into (3) and then into (6). By choice of $E(\tau)=(\rho(\theta)+\beta(\theta))\tau$, that is a linear rate envelope slackened by a rate $\beta(\theta)>0$, it follows for $\theta > 0$ that

$$\begin{aligned}\mathsf{M}_{A\oslash E}(\theta,t) &\leq \sum_{\tau=0}^{t-1} e^{\theta(\sigma(\theta)+\rho(\theta)(t-\tau))} e^{-\theta E(t-\tau)} \\ &\leq \sum_{\tau=1}^{\infty} e^{\theta(\sigma(\theta)+\rho(\theta)\tau)} e^{-\theta E(\tau)} \\ &\leq e^{\theta\sigma(\theta)} \int_0^{\infty} e^{-\theta\beta(\theta)\tau} d\tau \\ &= \frac{e^{\theta\sigma(\theta)}}{\theta\beta(\theta)}. \end{aligned} \tag{10}$$

In the second step we let $t \to \infty$ to compute a bound for any $t \geq 0$. In the third step, since $e^{-\theta\beta(\theta)\tau}$ is non-increasing in τ, each summand can be bounded by an integral of unit width left of the summand. Hence, the sum $\sum_{\tau=1}^{\infty}(\cdot)$ is bounded from above using the integral $\int_0^{\infty}(\cdot)d\tau$. Since $\beta(\theta) > 0$, the integral is finite. Finally, by application of Chernoff's theorem the transition from point A2 to B2 in Fig. 1 is made, yielding a solution of (4) for any $t \geq 0$ and $\theta > 0$ as

$$\mathsf{P}[A \oslash E(t) > b] \leq \frac{e^{\theta\sigma(\theta)} e^{-\theta b}}{\theta\beta(\theta)} = \varepsilon^s(b). \tag{11}$$

The result (11) immediately yields statistical performance bounds. For example, given a constant rate server with capacity C the backlog is bounded by (8) such that by insertion of $E(\tau) = C\tau$ into (11) the backlog bound $\mathsf{P}[B > b] \leq \varepsilon^s(b)$ is computed for $(\sigma(\theta), \rho(\theta))$ arrivals characterized by (9). From $E(\tau) = (\rho(\theta) + \beta(\theta))\tau$ in (10) the free parameter $\beta(\theta)$ is determined as $\beta(\theta) = C - \rho(\theta)$, where the condition $\beta(\theta) > 0$ implies the stability condition $\rho(\theta) < C$. Finally, the parameter $\theta > 0$ can be optimized to minimize $\varepsilon^s(b)$. Analogously, a FIFO delay bound W is found as $\mathsf{P}[W > b/C] \leq \varepsilon^s(b)$ with identical violation probability $\varepsilon^s(b)$.

Next, we review the relation of the exponentially bounded burstiness (EBB) envelope by Yaron and Sidi [10] to the $(\sigma(\theta), \rho(\theta))$ traffic model. This relation has been elaborated, e.g., in [18]. The EBB envelope is defined as

$$\mathsf{P}[A(\tau,t) - \rho(t-\tau) > b] \leq \alpha e^{-\theta b}. \tag{12}$$

The definition satisfies (1) where $E(\tau) = \rho\tau$ is a linear rate envelope. The model comprises parameters ρ, α, and $\theta \geq 0$ that can be directly related to the $(\sigma(\theta), \rho(\theta))$ traffic model by Chernoff's theorem. To this end, a transition from A1 to B1 in Fig. 1 is performed by insertion of (9) into (2). It follows for $\theta \geq 0$ that

$$\mathsf{P}[A(\tau,t) - \rho(\theta)(t-\tau) > b] \leq e^{\theta\sigma(\theta)} e^{-\theta b} \tag{13}$$

such that $\alpha = e^{\theta\sigma(\theta)}$ [18] and $\rho = \rho(\theta)$ is a function of θ. Using the EBB envelope, we next solve (4) corresponding to a transition from B1 to B2 in Fig. 1. In accordance with [10], [13], [14] we derive for $\theta > 0$ that

$$\begin{aligned}\mathsf{P}[A \oslash E(t) > b] &\leq \sum_{\tau=0}^{t-1} \mathsf{P}[A(\tau,t) - E(t-\tau) > b] \\ &\leq \sum_{\tau=1}^{\infty} e^{\theta\sigma(\theta)} e^{-\theta(b+\beta(\theta)\tau)} \\ &\leq e^{\theta\sigma(\theta)} e^{-\theta b} \int_0^{\infty} e^{-\theta\beta(\theta)\tau} d\tau \\ &= \frac{e^{\theta\sigma(\theta)} e^{-\theta b}}{\theta\beta(\theta)} = \varepsilon^s(b). \end{aligned} \tag{14}$$

The first step employs the union bound from (7). In the second step we insert the envelope $E(\tau) = (\rho(\theta) + \beta(\theta))\tau$ and use the EBB definition from (12), where we substitute $b + \beta(\theta)\tau$ for b and let $\alpha = e^{\theta\sigma(\theta)}$ from (13). Here, the sample path envelope $E(t-\tau)$ is a linear rate envelope relaxed by a slack rate $\beta(\theta) > 0$. This slack rate is crucial for the calculation of a sample path violation probability $\varepsilon^s(b)$. In the third step we let $t \to \infty$ and use the fact that the violation probability is a non-increasing function in time to bound each summand by an integral. Hence, the sum $\sum_{\tau\geq 1}^{\infty}(\cdot)$ is bounded from above using the integral $\int_0^{\infty}(\cdot)d\tau$. The sample path violation probability $\varepsilon^s(b)$ is found by evaluating the integral. This outcome implies the condition $\beta(\theta) > 0$, for the derivation of a finite $\varepsilon^s(b)$. Note that although the order of the individual steps differs the result (14) is identical to (11) [18].

Next, we present a random traffic source, that we use throughout this paper for numerical illustration of statistical multiplexing effects.

Example: Discrete Time On-off-source: We consider Markov sources with two states: state 1 (off) and state 2 (on). In the off state the source produces no traffic and in the on state the source produces traffic with a peak rate P. The steady state probability of the on state is $p_{on} = p_{12}/(p_{12} + p_{21})$ where p_{ij} is the transition probability from state i to state j. The mean rate of the source is $\lambda = p_{on}P$. Note that the on-off-source produces traffic with a certain burstiness, which is characterized by parameter $T = 1/p_{12} + 1/p_{21}$, that is the mean time to change states twice, i.e., the larger T the higher the burstiness of the source. The MGF of such an on-off-source is upper bounded by

$$\mathsf{M}_A(\theta,\tau) \leq e^{\theta\rho(\theta)\tau}$$

with $\rho(\theta)$ given in [23] as

$$\frac{1}{\theta}\log\left(\frac{p_{11}+p_{22}e^{\theta P}+\sqrt{(p_{11}+p_{22}e^{\theta P})^2-4(p_{11}+p_{22}-1)e^{\theta P}}}{2}\right)$$

for $\theta \geq 0$, where $\rho(\theta)$ lies between the peak and the mean rate of one source. Note that $\rho(\theta)$ is a function of θ that is fully determined by the traffic parameters λ, P and T.

Next, we display delay bounds for an on-off-source characterized by $P = 120$ Mbps, $\lambda = 20$ Mbps, and different burstiness parameters T at a constant rate link with capacity $C = 100$ Mbps. Since we use a model with slotted time we have to fix the duration of a time slot for numerical computations. Throughout this work, we choose a time slot of 0.1 ms that corresponds to the transmission time of a 10 kb, respectively, 1250 Byte sized packet. For numerical

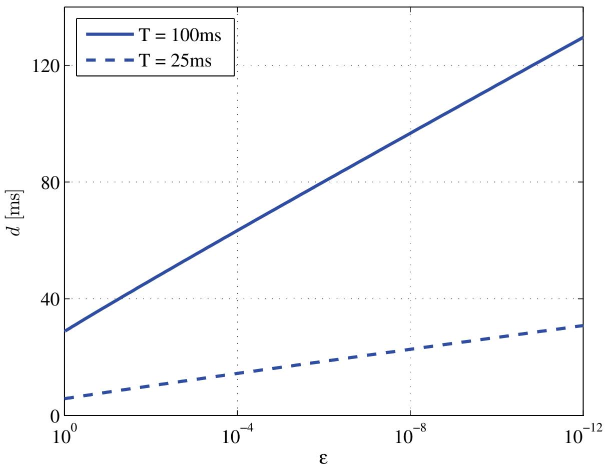

Fig. 2. Delay bounds for an on-off-source with different source burstiness T. The violation probability ε of the delay bound d decays exponentially fast where the slope is determined by the burstiness of the source.

computation we let parameter $\beta(\theta) = C - \rho(\theta)$ and optimize $\theta > 0$ to obtain the minimal delay bound. The results, displayed in Fig. 2, clearly show the exponential decay of the violation probability, as the delay bound is linear on the depicted log-scale. This result is obtained by any of the two methods presented before, i.e., either from the EBB envelope model or from the $(\sigma(\theta), \rho(\theta))$ MGF bound.

In this section we showed the derivation of performance bounds using affine envelopes. We presented two closely related traffic models, i.e., $(\sigma(\theta), \rho(\theta))$ and EBB, on which we base our subsequent investigations. Both models can be related to Fig. 1. On the one side the arrival MGF bound in (9) can be inserted at point A1. On the other side the EBB model from (12) is resembled in point B1. Further, we presented a $(\sigma(\theta), \rho(\theta))$, respectively, EBB class traffic source, i.e., the on-off-source model, that will be deployed in examples of statistical multiplexing effects throughout this work. In the next section, we make use of the presented foundation to derive performance bounds under statistical multiplexing of independent arrival flows.

III. Statistical Multiplexing

In Sect. II, we reviewed fundamental traffic models and respective methods to derive statistical performance bounds, e.g., on backlog and delay. We examined the relation between these models and illustrated how they can be transformed into each other. Interestingly, while the different traffic models provide identical results if a single flow is considered, we will show in this section that such an equivalence does not hold in case of statistical multiplexing. We will model individual flows by any of the four traffic models depicted in Fig. 1 to systematically compare performance bounds that can be derived thereof for an aggregate of independent flows. The analytical procedure is structured as following:

(i) choose a traffic model to characterize a single flow. As described in Sect. II-A, a flow can be characterized by any of the four models A1, A2, B1, and B2 depicted in Fig. 1;

(ii) consider the aggregate of independent flows each characterized as in (i);

(iii) derive performance bounds for the aggregate traffic.

Again, we use Fig. 1 to illustrate this procedure. First, (i) navigate to the desired single flow characterization, A1, A2, B1, or B2. Next, (ii) consider the superposition of multiple independent flows of that type. Finally, (iii) continue navigating until you reach the performance bound $\mathsf{P}[B > b]$.

In general, we consider the aggregate of N independent stationary arrival flows indexed $i \in [1, N]$ of the form

$$A_{ag}(t, t+\tau) = \sum_{i=1}^{N} A_i(t, t+\tau).$$

Analogously, we define the sum of all traffic envelopes

$$E_{ag}(\tau) = \sum_{i=1}^{N} E_i(\tau).$$

The superposition of traffic flows is essentially an addition of random processes, respectively, random variables that can be dealt with in two basic ways: It is generally known for sums of independent random variables that the MGF of the sum is composed by the multiplication of the individual MGFs; it is also known that the probability density function (PDF) of the sum is composed by the convolution of the individual PDFs. The duality of the two concepts, that is due to the properties of the Laplace transform, is proven for example in [24]. The first method can be applied when a flow is characterized by an MGF (points A1, A2), while the latter is applicable when a flow is characterized by an envelope function (points B1, B2).

A. Multiplexing Traffic modeled by MGFs

We analyze aggregate traffic that is modeled by MGFs. We follow the steps $(i) - (iii)$ described above. First, we assume each of the arrival flows $A_i(t, t+\tau)$ with $i \in [1, N]$ possesses a $(\sigma(\theta), \rho(\theta))$ MGF bound (9). This corresponds to a characterization of individual flows at point A1 in Fig. 1.

It is known that the MGF of a sum of two independent random variables $X_1 + X_2$ is given as $\mathsf{M}_{X_1+X_2} = \mathsf{M}_{X_1}\mathsf{M}_{X_2}$. Hence, the MGF of the aggregate traffic is given by multiplication of the individual MGFs as

$$\begin{aligned}\mathsf{M}_{\sum_i A_i - \sum_i E_i}(\theta, \tau) &= \prod_{i=1}^{N} \mathsf{M}_{A_i - E_i}(\theta, \tau) \\ &= \left(\mathsf{M}_{A_i - E_i}(\theta, \tau)\right)^N \end{aligned} \tag{15}$$

for all $\theta \in \mathbb{R}$ and $\tau \geq 0$. In the second step we simplified the expression for homogeneous arrival flows. We consider the homogeneous case throughout this work if not specified otherwise. Heterogeneous flows can be analyzed in the same way, however, at the expense of additional notation. We use the $(\sigma(\theta), \rho(\theta))$ MGF bound (9) to find from (15) that

$$\begin{aligned}\mathsf{M}_{\sum_i A_i - \sum_i E_i}(\theta, \tau) &\leq e^{N\theta(\sigma(\theta)+\rho(\theta)\tau - E_i(\tau))} \\ &= e^{N\theta(\sigma(\theta)-\beta(\theta)\tau)}, \end{aligned} \tag{16}$$

where we set the envelope of a single flow to $E_i(\tau) = (\rho(\theta) + \beta(\theta))\tau$. From (16) we calculate the sample path violation probability $\varepsilon^s(b)$ for N homogeneous $(\sigma(\theta), \rho(\theta))$ traffic flows. Along the same line as the derivation of (10) and (11) in Sect. II-B we first derive $\mathsf{M}_{(\sum_i A_i)\oslash(\sum_i E_i)}(\theta, t)$ from (16) and then use Chernoff's theorem to obtain for $\theta > 0$ that

$$\mathsf{P}\big[\big(\textstyle\sum_i A_i\big) \oslash \big(\sum_i E_i\big)(t) > b\big] \leq \frac{e^{N\theta\sigma(\theta)}e^{-\theta b}}{N\theta\beta(\theta)}. \tag{17}$$

Note that the order of applying Chernoff's theorem and the union bound does not affect the derivation of (17).

Given a work conserving server with capacity C, we can insert $\sum_i E_i(\tau) = C\tau$ and immediately obtain backlog and delay bounds from (17). Since $E_i(\tau) = (\rho(\theta) + \beta(\theta))\tau$ this implies spare capacity, respectively, the stability condition $C - N\rho(\theta) = N\beta(\theta) > 0$, which is necessary to derive finite performance bounds.

As an alternative, we regard traffic flows that are each modeled by MGFs of a sample path argument, i.e., $\mathsf{M}_{A\oslash E}(\theta, t)$, for example (10). This corresponds to a characterization of individual flows at point A2 in Fig. 1.

The sum of N independent random variables of the type of $A_i \oslash E_i(t)$ for $i \in [1, N]$ results in a multiplication of the corresponding MGFs given for all $\theta \in \mathbb{R}$ and $t \geq 0$ as

$$\begin{aligned} \mathsf{M}_{\sum_i(A_i\oslash E_i)}(\theta, t) &= \prod_{i=1}^{N} \mathsf{M}_{A_i\oslash E_i}(\theta, t) \\ &= (\mathsf{M}_{A_i\oslash E_i}(\theta, t))^N, \end{aligned} \tag{18}$$

where in the second line we again assume homogenous flows. By insertion of (10) into (18) it follows with Chernoff's theorem for $\theta > 0$ that

$$\mathsf{P}\big[\textstyle\sum_i (A_i \oslash E_i)(t) > b\big] \leq \frac{e^{N\theta\sigma(\theta)}e^{-\theta b}}{(\theta\beta(\theta))^N}. \tag{19}$$

First of all, it becomes obvious that the quantity that is estimated by (19) differs from (17). It holds, however, that

$$\mathsf{P}\big[\big(\textstyle\sum_i A_i\big) \oslash \big(\sum_i E_i\big)(t) > b\big] \leq \mathsf{P}\big[\sum_i (A_i \oslash E_i)(t) > b\big] \tag{20}$$

such that (19) provides an upper bound for the expression on the left hand side of (17). The form on the left hand side in (17) is desired since it immediately yields performance bounds, e.g., it resembles the backlog formula (8). To verify (20) expand the $\oslash$ operator and note that it is generally true that

$$\sup_{\tau}\big\{\textstyle\sum_i A_i(\tau, t) - E_i(t-\tau)\big\} \leq \sum_i \sup_{\tau}\{A_i(\tau, t) - E_i(t-\tau)\}.$$

Regarding the derivation of (17) and (19) a similar argument yields for $\theta \geq 0$ that

$$\mathsf{M}_{(\sum_i A_i)\oslash(\sum_i E_i)}(\theta, t) \leq \mathsf{M}_{\sum_i(A_i\oslash E_i)}(\theta, t), \tag{21}$$

where the left and the right hand side are the MGFs that are used in (17) and (19), respectively. This relation leads to preferring traffic model A1 over A2 for the superposition of flows since it leads to a smaller MGF of the multiplexed traffic, which leads in turn to tighter performance bounds after invoking Chernoff's theorem. The result is intuitive as A1 exploits statistical independence of arrival flows at *every* point in time, unlike A2 which only exploits the statistical independence of *entire* sample paths of arrival flows. While (21) provides a general statement for the MGFs that are involved, we note that the solutions in (17) and (19) use $(\sigma(\theta), \rho(\theta))$ MGF bounds as well as the union bound. A relation of the right hand sides of (17) and (19) similar to (21) is not derived here. Note that the parameter $\theta > 0$ can be optimized to minimize the right hand side of (17) and (19) individually.

B. Multiplexing Traffic modeled by Envelopes

Next, we look into traffic that is characterized by envelope functions, i.e., using bounds on the CCDF. This corresponds to a representation of traffic at the points B1 or B2 on Fig. 1. Generally, the superposition of traffic flows characterized by CCDF bounds is captured using the Stieltjes convolution as described in [10], [25].

Consider two independent random variables X_1 and X_2 with respective cumulative distribution functions (CDFs) F_{X_i} and respective CCDFs $\varepsilon_i = 1 - F_{X_i}$ for $i \in [1, 2]$. It is generally known that $F_{X_1+X_2}(b) = (F_{X_1} * F_{X_2})(b) = \int_{-\infty}^{\infty} F_{X_1}(b-a)dF_{X_2}(a)$. The right hand side is the definition of the Stieltjes convolution. We slightly abuse notation and write $\varepsilon_1 * \varepsilon_2(b)$ as a shorthand for $1 - F_{X_1} * F_{X_2}(b)$, i.e., the CCDF of the sum $X_1 + X_2$.

The next lemma provides an improvement of an earlier multiplexing result from [10].

Lemma 1 (EBB multiplexing)**.** *Given two independent random variables X_1, X_2 with CCDFs*

$$\varepsilon_i(b) = \begin{cases} \alpha e^{-\theta b} & \text{for } b \geq b^* = \frac{1}{\theta}\log\alpha \\ 1 & \text{else} \end{cases}$$

for $i \in [1, 2]$. For $b \geq 2b^*$ it holds that

$$(\varepsilon_1 * \varepsilon_2)(b) = (1 + \theta b - 2\log\alpha)\,\alpha^2 e^{-\theta b}$$

For random variables with CCDF bounds $\varepsilon_i(b) \leq \alpha e^{-\theta b}$ for $i \in [1, 2]$, it holds for $b \geq 2b^*$ that

$$(\varepsilon_1 * \varepsilon_2)(b) \leq (1 + \theta b - 2\log\alpha)\,\alpha^2 e^{-\theta b}.$$

We provide the proof of Lem. 1 in the appendix. Note that $\varepsilon_i(b)$ is the exponential CCDF if $\alpha = 1$. If $\alpha > 1$, $\varepsilon_i(b)$ is a CCDF only for $b \geq b^*$, where b^* is given in Lem. 1. For the special case $\alpha = 1$ Lem. 1 recovers the well-known Erlang distribution. In addition, one can deduce from Lem. 1 that the violation probability for the superposition of two EBB flows is not EBB. The last equation in Lem. 1 is similar to Lem. 6 from [25] pp.199, however, it gives a closed form expression for $\varepsilon_i(b) \leq \alpha e^{-\theta b}$.

Now, we consider the superposition of independent traffic flows $i \in [1, N]$ with envelopes $E_i(\tau)$ according to (1). In terms of Fig. 1 this corresponds to characterizing each individual flow at point B1. We choose $E_i(\tau) = (\rho(\theta) + \beta(\theta))\tau$ and use the EBB definition from (12), where we substitute $b + \beta(\theta)\tau$ for b and let $\alpha = e^{\theta\sigma(\theta)}$ from (13), to arrive at

$$\mathsf{P}\left[A_i(t, t+\tau) - E_i(\tau) > b\right] \leq e^{\theta\sigma(\theta)}e^{-\theta\beta(\theta)\tau}e^{-\theta b}. \tag{22}$$

As before $\beta(\theta)$ is a slack rate that is used to achieve a decaying and integrable violation probability.

Next, we calculate the violation probability $\varepsilon^p(b)$ for the superposition of traffic flows by self-convolution of the right hand side of (22). We first consider $N = 2$ flows. Later, we show how the result can be generalized for more flows by repeated application. We employ Lem. 1 with $\varepsilon_i^p(b)$ given as the right hand side of (22). Precisely, substitute α in Lem. 1 with $e^{\theta\sigma(\theta)}e^{-\theta\beta(\theta)\tau}$. We take the result from Lem. 1 and invoke the union bound as in the derivation of (14) to obtain the sample path violation probability $\varepsilon^s(b)$. As before, we upper bound the sum $\sum_{\tau=1}^{\infty}(\cdot)$ by the integral $\int_0^{\infty}(\cdot)d\tau$ and find for $b \geq 2\sigma(\theta)$ and $\theta > 0$ that

$$\mathsf{P}\left[(A_1+A_2)\oslash(E_1+E_2)(t)>b\right] \leq \left(2+\theta\left(b-2\sigma\left(\theta\right)\right)\right)\frac{e^{2\theta\sigma(\theta)}e^{-\theta b}}{2\theta\beta(\theta)}. \quad (23)$$

The derivation of (23) is given in the appendix. We can set the sum of the envelopes $\sum_i E_i(\tau) = C\tau$, to readily find backlog and delay bounds at a constant rate server with capacity C.

Observe that the MGF model (17) yields a tighter sample path violation probability than the convolution method (23), where $N = 2$, since the additional prefactor in (23) is generally larger than one. One can show that the application of Chernoff's theorem once as in the derivation of (17) is tighter than using it twice as in the derivation of (23).

If the CCDF for each flow is a priori given, Lem. 1 provides an exact result for the CCDF of the multiplexed flows. Note, however, that non-trivial examples exist, which show that it is generally not possible to construct an envelope $E(\tau)$ such that (1) holds with equality for all $b \geq 0$ and $\tau \geq 0$.

Finally, we regard independent flows that are characterized by sample path envelopes, i.e., using a representation at point B2 in Fig. 1. We consider first two homogeneous EBB traffic flows with individual sample path violation probabilities $\varepsilon_i^s(b)$ as derived in (14). The superposition of such flows implies an application of the convolution operation to sample path violation probabilities $\varepsilon^s(b)$ as proposed in [25] pp. 134. We resort to Lem. 1 for the convolution of $\varepsilon_i^s(b)$. It follows that the sample path violation probability for the multiplexed traffic is bounded for $\theta > 0$ as

$$\mathsf{P}\left[(A_1\oslash E_1)+(A_2\oslash E_2)(t)>b\right] \leq \left(1+\theta\left(b-2\sigma\left(\theta\right)\right)+2\log\left(\theta\beta(\theta)\right)\right)\frac{e^{2\theta\sigma(\theta)}e^{-\theta b}}{(\theta\beta(\theta))^2}. \quad (24)$$

The derivation of (24) is given in the appendix. Both (23) and (24) exhibit the same exponential tail decay. From (20) we deduce that the right hand side from (24) is also an upper bound for the left hand side of (23), wherefrom performance bounds follow immediately.

Next, we present solutions for $N > 2$ flows. To this end, the following lemma provides an EBB characterization for superposed EBB flows. The idea dates back to [10] where, however, no explicit bound is calculated. The usefulness of the result is due to the fact that it dispenses with the polynomial on the right hand side of Lem. 1 such that Lem. 1 can be used repeatedly.

Lemma 2 (EBB type bound for multiplexed EBB flows)**.** *Given Lem. 1. It holds that*

$$\left(1+\theta b-2\log\alpha\right)\alpha^2 e^{-\theta b} \leq K e^{-(\theta-\phi)b},$$

where $\phi \in (0,\theta)$ is a free parameter and

$$K = \frac{\theta}{\phi}\left(\frac{\alpha^2}{e}\right)^{\frac{\theta-\phi}{\theta}}.$$

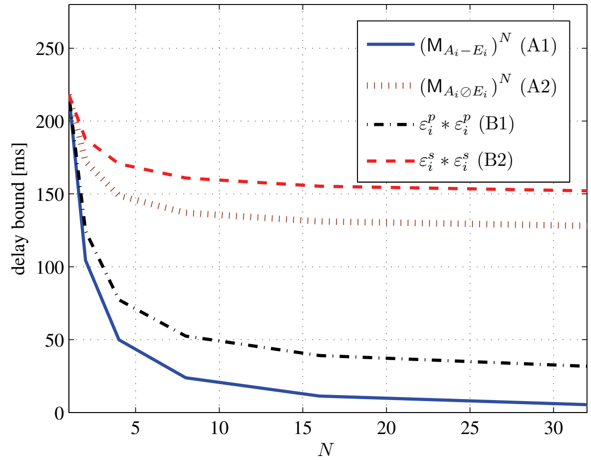

Fig. 3. Statistical delay bounds for an aggregate of N independent flows. The mean and peak arrival rates of the aggregate are fixed. The delay bounds differ depending on the traffic model, i.e., A1, A2, B1 and B2 from Fig. 1. The violation probability ε^s is fixed to 10^{-3}.

Lem. 2 states that an EBB type bound on the violation probability for multiplexed EBB traffic exists, if the decay exponent is degraded by a free parameter $0 < \phi < \theta$. The proof of Lem. 2 is given in the appendix.

Lem. 2 can be used to combine $N = 2^k$ independent EBB flows each characterized by (22), where $k \in \mathbb{N}$. This is carried out by repeatedly invoking Lem. 1 and Lem. 2. Accordingly, we extend (23) from two to N flows. We obtain

$$\mathsf{P}\left[\left(\textstyle\sum_i A_i\right)\oslash\left(\textstyle\sum_i E_i\right)(t)>b\right] \leq H_k\frac{e^{N(\theta-\phi)\sigma(\theta)}}{(\theta-k\phi)N\beta(\theta)}e^{-(\theta-k\phi)b}, \quad (25)$$

where $\theta > 0$ and $\phi \in (0,\theta/k)$ are free parameters. Similarly, using the traffic model at point B2 for each flow we extend (24) from two to N flows such that it holds for $\theta > 0$

$$\mathsf{P}\left[\textstyle\sum_i(A_i\oslash E_i)(t)>b\right] \leq H_k\left(\frac{e^{\theta\sigma(\theta)}}{\theta\beta(\theta)}\right)^{N\frac{\theta-k\phi}{\phi}} e^{-(\theta-k\phi)b}. \quad (26)$$

The derivations of (25) and (26) as well as the parameter H_k can be found in the appendix. For the quantity on the left hand side of (26) the same discussion applies as for (24). Backlog and delay bounds at a constant rate server with capacity C follow as before by setting $\sum_i E_i(\tau) = C\tau$.

In Fig. 3 we show numerical examples that compare delay bounds achieved by the different methods for the superposition of independent flows. We plot delay bounds with violation probability $\varepsilon^s = 10^{-3}$ for N multiplexed on-off-sources at a constant rate server with capacity $C = 100$ Mbps. We keep the aggregate mean arrival rate and peak rate constant and fix the parameters of the individual sources as $\lambda = 60/N$ Mbps, $P = 120/N$ Mbps, and $T = 100$ ms. The free parameter $\theta > 0$ is optimized numerically for each of the methods individually.

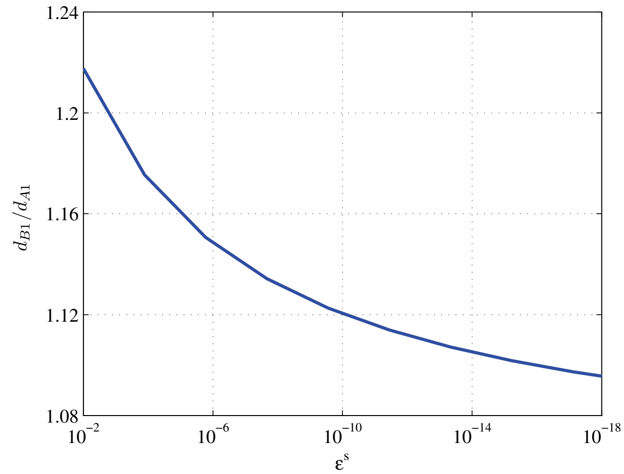

Fig. 4. Delay bounds d_{B1} obtained from (23) relative to the delay bound d_{A1} from (17) for $N = 2$ multiplexed flows. While d_{A1} is tighter than d_{B1}, the two results converge for $\varepsilon^s \to 0$.

The statistical multiplexing gain is apparent in the decay of the delay bounds with the number of multiplexed flows. The delay bounds shown are obtained for traffic characterized by A1, A2, B1, or B2. The respective equations for A1 and A2 are (17) and (19). The equations for B1 and B2 are for $N = 2$ (23) and (24) and for $N > 2$ (25) and (26). The curves are obtained by plugging the model parameters into the given closed form expressions and optimizing numerically.

Fig. 3 shows a considerable advantage of A1 and B1, where statistical independence is considered at any point in time, over A2 and B2, that use a sample path traffic model for multiplexing. This is expected from (20) and (21). While the traffic model B2 is inferior to the other methods, we note that in certain, important cases conditions may arise where sample path arguments are required such that model B1 cannot be applied. One such case are multi-node networks, see Sect. V.

Notably, Fig. 3 shows that a calculation based on MGFs (A1) yields tighter bounds than the envelope-based method (B1). One reason for the deviation at B1 is due to the CCDF bounds that are obtained from Chernoff's theorem. Chernoff's theorem delivers tighter bounds for smaller violation probabilities. We consider first the case $N = 2$, where we can resort to (23) for calculation without including Lem. 2. In this case, it can be shown that the relative ratio of the delay bounds d_{B1}/d_{A1} converges to 1 for $\varepsilon \to 0$, respectively, $d_{(\cdot)} \to \infty$. Here, $d_{(\cdot)}$ denotes the delay bound obtained by model $(\cdot)$. Fig. 4 displays the ratio d_{B1}/d_{A1} versus ε^s for $N = 2$. Clearly, d_{B1}/d_{A1} decreases for smaller ε^s. For $N > 2$ the results for B1 in Fig. 3 are obtained from (25) that is conservative due to the application of Lem. 2.

While MGFs provide an elegant and accurate way to analyze multiplexed independent flows, they lead to cumbersome expressions if independence cannot be assumed, see [15] for discussion. In contrast, envelope functions provide simple solutions for this case, where multiplexing without independence is expressed by a different type of convolution. In detail, $\varepsilon_1 * \varepsilon_2$ as in Lem. 1 is replaced by $\varepsilon_1 \otimes \varepsilon_2$ where the operator $\otimes$ denotes the min-plus convolution $f \otimes g(t) = \inf_{\tau\in[0,t]} \{f(\tau) + g(t-\tau)\}$. For the EBB model it follows that $\mathsf{P}[(\sum_i A_i) \oslash (\sum_i E_i)(\tau) > b] = \mathsf{P}[\sum_i (A_i \oslash E_i)(\tau) > b] \le N e^{\theta\sigma(\theta)} e^{-\theta b/N}/(\theta\beta(\theta))$, i.e., traffic models B1 and B2 deliver the same results if independence is not assumed.

In this section we showed the impact of the traffic model on performance bounds derived thereof. We analyzed the assumptions of each model and compared the resulting bounds. We particularly looked at two different aspects. First, calculation using either the MGFs of traffic arrivals or envelopes derived from MGFs. Secondly, invoking the independence of the arrivals at every point in time or for entire sample paths. We find that all methods deliver the same exponential tail decay as they resort to Chernoff's theorem. The tightness of bounds derived from the four models differs, however, substantially with increasing number of flows, see Fig. 3. We conclude that pointwise arguments are superior if independent traffic flows are multiplexed, i.e., models A1 and B1. Moreover, if traffic flows are characterized by MGFs or MGF bounds, the superposition of flows is accomplished best by multiplication of the MGFs, i.e., model A1. We will in the sequel consider this model if not stated otherwise. We conclude this section with an application to the dimensioning of, e.g., access multiplexers.

C. An Application to Dimensioning

A common dimensioning problem in access networks such as DSL access multiplexers is to determine the number of subscribers, respectively, flows N that can be admitted given a certain capacity C and buffer space b. Typically, a deterministic, worst-case allocation $\sum_i P_i \le C$ that considers the peak rates P_i of incoming flows is to costly, whereas an allocation $\sum_i \lambda_i \le C$ that resorts only to the average rates λ_i will be to optimistic and will frequently result in congestion. For this reason, the solution to the dimensioning problem has to take QoS constraints, such as the probability of buffer overflow $\mathsf{P}[B > b]$ or the probability of excessive queuing delays $\mathsf{P}[W > d]$, into account. Both quantities follow readily from the theory presented so far. In the following we show numerical results on the number of flows N that can be admitted such that a delay bound of $d = 100$ ms is exceeded at most with probability $\varepsilon^s = 10^{-3}$. The incoming traffic is generated by homogenous on-off-sources as described in Sect. II with following parameters: $P = 120$ Mbps, $\lambda = 20$ Mbps, and burstiness parameter $T = 100$ ms.

In Fig. 5(a) we vary the link capacity C and show how many flows N can be admitted at most without violating the QoS constraint. The dashed lines show the mean rate allocation $N = \lfloor C/\lambda \rfloor$ as well as the peak rate allocation $N = \lfloor C/P \rfloor$. The solid line represents N as obtained from (17). Fig. 5(a) shows that the number of admissible flows is much higher than in case of the deterministic peak rate allocation if a small probability of QoS violation ε^s is tolerated. Note that the mean rate allocation only achieves system stability without any QoS guarantees. With increasing N the aggregate traffic becomes, however, smoother due to statistical multiplexing such that the resources that are required per flow approach the average rate. This effect is illustrated in Fig. 5(b) where the number of admissible flows per unit of capacity N/C approaches the

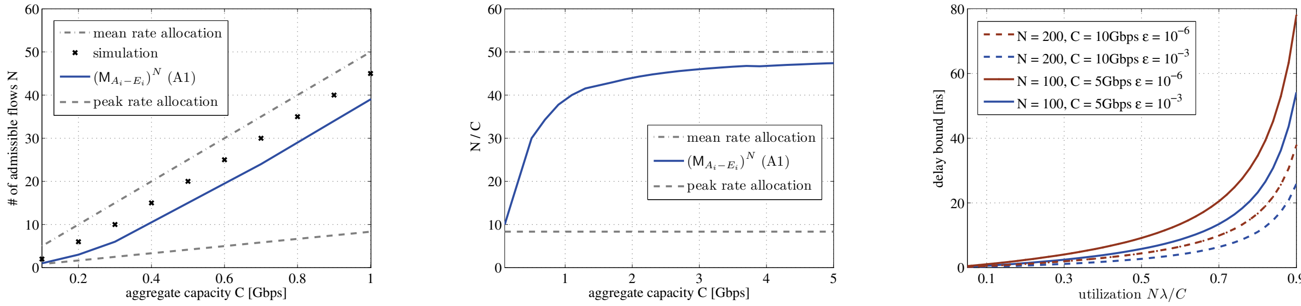

(a) Number of admissible flows (b) Flows per unit capacity (c) Delay bound vs. utilization

Fig. 5. Statistical multiplexing gain as accomplished by traffic model A1 from Fig. 1. (Left) With $\varepsilon^s = 10^{-3}$ much more flows can be admitted than in case of the deterministic peak rate allocation. The mean rate allocation indicates the border of system stability without providing any QoS guarantees. (Middle) The number of admissible flows per unit capacity C converges towards the mean rate allocation, showing significant economies of scale. (Right) The larger multiplexing gain of $N = 200$ vs. $N = 100$ flows leads to smaller delay bounds at the same utilization.

mean rate allocation of 50 flows per Gbps. Fig. 5(a) also shows simulation results on the maximum number of admitted flows under the same delay percentile constraint. The simulation was carried out using the network simulator ns-2 [26]. From Fig. 5(a) it is clear that the analytical calculation at A1 yields results that are close to the simulations.

Fig. 5(c) depicts the link utilization $N\lambda/C$ and the corresponding delay bound for fixed ε^s. For each curve N and C are fixed and λ is varied. The solid lines compare the delay bound variation for two different violation probabilities $\varepsilon^s = \{10^{-3}, 10^{-6}\}$. The dashed lines show the statistical gain, in terms of the delay bound, if the capacity is increased from 5 to 10 Gbps. Note that the utilization is identical, before and after increasing C, through adapting N from 100 to 200 flows.

IV. Scheduling and Leftover Service Curves

So far, we considered an aggregate of flows that all receive the same service from the network. In this section, we investigate scheduling of different types of flows. Scheduling is used to provide different levels of QoS, e.g., to prioritize voice and video traffic over best-effort traffic. Interestingly, a statistical gain is present also between different types of flows at a scheduler if independence holds [15].

Fig. 7 introduces the notation, where we deal with the single node case here. We consider a through traffic flow $A^{th}(t)$ and a cross traffic flow $A_1^{cr}(t)$, respectively. Using the traffic models from Sect. III the flows $A^{th}(t)$ and $A_1^{cr}(t)$ can be easily extended to an aggregate of flows. To characterize the service that is available to the through traffic flow we use so called leftover service curves from the stochastic network calculus. While models for a large number of schedulers are available, see e.g. [8], [22], we restrict the exposition to a general scheduling model that assumes no particular order of scheduling. The model applies to priority scheduling where the cross traffic has priority. It is conservative for other work-conserving scheduling disciplines.

A. Leftover Service Curves using MGFs

First, we regard a service curve model, where the service is viewed as a random process that can be specified using MGFs [15], [23]. The framework uses the notion of dynamic servers [23] that relates the arrival process $A(t)$ of a server to its departure process $D(t)$ by a bivariate random process, respectively, service curve $S(\tau, t)$ as

$$D(t) \geq A \otimes S(t) := \inf_{\tau \in [0,t]} \{A(\tau) + S(\tau, t)\} \qquad (27)$$

for all $t \geq 0$. An example of a dynamic server is a link with a time varying capacity, e.g., a wireless link, where $S(\tau, t)$ specifies the service that is available in any interval $[\tau, t)$ [23].

Given a dynamic server $S(\tau, t)$ with through and cross traffic, a service curve left over by the cross traffic is [15]

$$S^{lo}(\tau, t) = [S(\tau, t) - A^{cr}(\tau, t)]_+, \qquad (28)$$

where $[x]_+ = \max\{0, x\}$ and the superscript lo denotes leftover. Regarding the through traffic arrivals $A^{th}(t)$ and departures $D^{th}(t)$, the leftover service curve $S^{lo}(t)$ from (28) satisfies (27), i.e., $D^{th}(t) \geq A^{th} \otimes S^{lo}(t)$.

We regard independent $(\sigma(\theta), \rho(\theta))$ cross traffic (9) at a constant rate work-conserving server with capacity C, respectively, service curve $S(t, t+\tau) = C\tau$ with MGF $\mathsf{M}_S(-\theta, \tau) = e^{-\theta C \tau}$. The MGF of the leftover service curve follows from (28) as [15]

$$\begin{aligned} \mathsf{M}_{S^{lo}}(-\theta, \tau) &\leq \min[1, \mathsf{M}_S(-\theta, \tau)\, \mathsf{M}_{A^{cr}}(\theta, \tau)] \\ &\leq e^{-\theta[(C - \rho^{cr}(\theta))\tau - \sigma^{cr}(\theta)]_+}. \end{aligned} \qquad (29)$$

Using the MGF of the through traffic arrivals and the MGF of the leftover service curve (29) statistical backlog and delay bounds can be computed from Th. 2 in [15]. The operation assumes statistical independence of the through traffic and the service, respectively, the cross traffic and employs a multiplication of the mentioned MGFs at each point in time. In terms of Fig. 1 this is comparable to multiplexing with traffic model A1.

B. Leftover Service Curves using Envelopes

Alternatively, a leftover service curve can be derived from envelope functions of the cross traffic. The model relies on so called statistical service curves $S(t)$ that are deterministic functions defined in [14] and similarly in [11] as

$$\mathsf{P}\left[D(t) < \inf_{\tau \in [0,t]} \left\{A(\tau) + [S(t-\tau) - b]_+\right\}\right] \leq \varepsilon(b). \qquad (30)$$

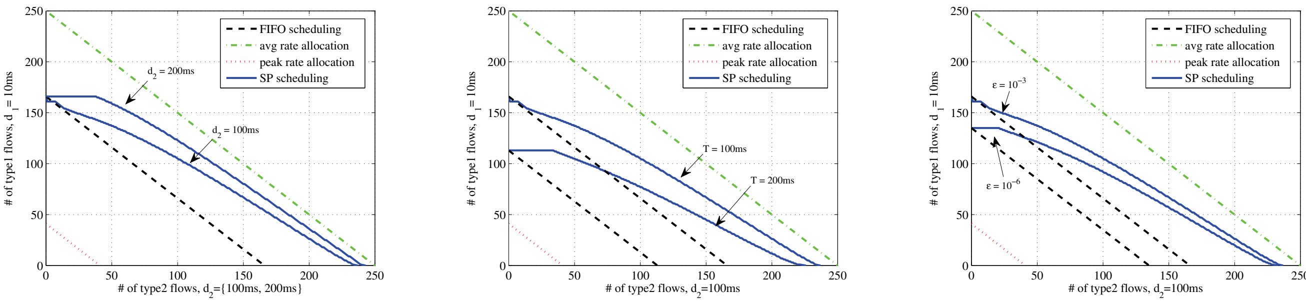

(a) Impact of the delay bound of type 2 flows d_2 (b) Impact of the source burstiness T (c) Impact of the violation probability ε

Fig. 6. Admission regions for type 1 and type 2 flows with different target delay bounds d_1 and d_2 with violation probability ε. FIFO scheduling without differentiation of flows is compared to SP scheduling, where type 1 flows have high and type 2 flows have low priority. SP scheduling permits admitting significantly more type 2 flows, the larger the delay bound d_2 is. We also show the average rate allocation, that denotes the stability boundary without any delay guarantees, and the peak rate allocation. Compared to the deterministic peak rate allocation, statistical multiplexing achieves a considerable improvement.

The definition (30) comprises a violation probability $\varepsilon(b)$ for $b \geq 0$, which is decreasing in b.

The leftover statistical service curve of a work-conserving constant rate server with capacity C follows by subtraction of the sample path envelope of cross traffic $E^{cr}(t)$ as [14]

$$S^{lo}(t) = Ct - E^{cr}(t). \tag{31}$$

Given through traffic, $S^{lo}(t)$ from (31) satisfies the definition of statistical service curve (30) where $\varepsilon(b)$ is given by the sample path violation probability $\varepsilon^s(b)$ (14) of the cross traffic envelope $E^{cr}(t)$. Given EBB cross traffic with affine sample path envelope $E^{cr}(\tau) = (\rho^{cr} + \beta^{cr})\tau$. A leftover service curve follows readily as $S^{lo}(t) = (C - \rho^{cr} - \beta^{cr})t$.

Based on the definition (30) performance bounds are derived in Th. 2 in [14]. For example, a backlog bound follows by substitution of $S^{lo}(t)$ for Ct in (8). The derivation of performance bounds builds on sample path envelopes for the through as well as for the cross traffic. An immediate extension to include statistical independence of through and cross traffic suggests the convolution of the sample path violation probabilities of the aforementioned envelopes, see [25] pp. 135. In terms of Fig. 1, this can be related to multiplexing at point B2.

C. An Application to Admission Control

Due to resource constraints and heterogeneous QoS demands, access networks frequently employ scheduling for service differentiation. To this end, it is important for a network service provider to determine the number of flows that can be admitted to each QoS class.

We show admission regions for two classes of traffic flows with different delay requirements, denoted type 1 and type 2 traffic, that can, e.g., be considered high priority voice and video traffic, respectively, best effort traffic. The admission regions indicate the number of admissible flows of type 1 and type 2, respectively, such that a certain admission criterion is not violated for each of the two types of flows. The admission criterion for type 1 flows is a target delay bound of $d_1 =$ 10 ms, while for type 2 flows it is $d_2 = 100$ ms, both subject to a violation probability of $\varepsilon = 10^{-3}$. Traffic flows of both types are generated by on-off-sources with peak rate $P =$ 120 Mbps, mean rate $\lambda = 20$ Mbps, and burstiness parameter $T = 100$ ms. The link has a capacity $C = 5$ Gbps. In case of scheduling, we applied (31) for computation of the leftover service curve after the type 1 flows are scheduled. The intra-class multiplexing of flows uses MGFs as in (16), i.e. point A1 in Fig. 1. For comparison we also show results for peak rate allocation $N = \lfloor C/P \rfloor$ and mean rate allocation $N = \lfloor C/\lambda \rfloor$, respectively. Note that in case of the mean rate allocation no QoS guarantees can be given.

Fig. 6 shows the benefit of statistical multiplexing in terms of larger admission regions (dashed and solid lines) compared to the peak rate allocation (dotted lines). The dashed lines mark admission regions for first-in first-out (FIFO) scheduling without differentiation of type 1 and type 2 flows. The solid lines show admission regions for static priority (SP) scheduling, where the type 1 flows have high priority. The advantage of scheduling is apparent as more low priority data flows of type 2 can be included. Note that without scheduling the smaller delay bound d_1 of the type 1 flows governs the admission region as long as at least one type 1 flow is in the system. In addition, Figs. 6(a), 6(b), and 6(c) show how the admission regions change in case of a variation of d_2, T, and ε, respectively. Depending on the parameters, low priority type 2 flows can be added even if the maximum number of high priority type 1 flows is in the system.

V. Convolution-form Networks

A main result of the network calculus is a natural extension of the service curve model from single to tandem nodes by min-plus convolution of the nodes' individual service curves. The result is an end-to-end service curve that models an entire so-called convolution-form network [17]. Similar, although more involved, results have also been obtained in the stochastic network calculus, which can in addition take advantage of the statistical independence of individual nodes, respectively, cross flows at these nodes [15]. The multi-node network that we consider in the sequel is illustrated in Fig. 7, where a tagged through flow traverses n consecutive work-conserving nodes with capacity C and independent cross flows. All flows can be aggregate flows that comprise a set of sub-flows. We consider homogeneous $(\sigma(\theta), \rho(\theta))$, respectively, EBB cross flows.

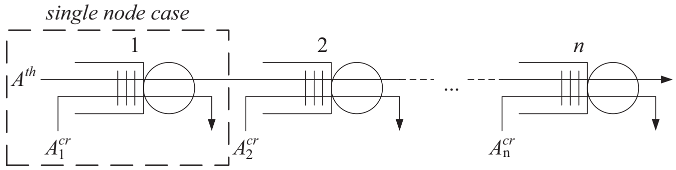

Fig. 7. A through flow traverses n nodes. At each node independent cross traffic is multiplexed and demultiplexed. All flows can be aggregate flows.

In the scenario depicted in Fig. 7 we can identify three types of independence assumptions contributing to the statistical multiplexing gain: i) between sub-flows within an aggregate flow, ii) between the aggregate through flow and the aggregate cross flows, and iii) between cross flows at consecutive nodes. The first can be utilized as in Sect. III either using the MGF or envelope functions. The second effect can be exploited as described in Sect. IV. Next, we look into the third case. In the sequel we will show the state of the art in considering statistical independence in multi-node scenarios. Next, we will show the fundamental assumptions behind different models, that provide multi-node performance bounds. Then, we derive a scaling behavior of end-to-end delay bounds for n tandem nodes with EBB cross traffic, when considering statistical independence using envelope functions. Finally, we compare the results of different models that incorporate statistical independence of cross traffic.

A. Convolution Gain in Tandem Networks using MGFs

The framework of stochastic network calculus using MGFs [15], [23] enables the derivation of end-to-end performance bounds under statistical independence of the service curves of the individual nodes. An MGF bound for the end-to-end service curve of the through flow as in Fig. 7 is obtained by convolution of the MGFs of the leftover service curves $\mathsf{M}_{S_i^{lo}}(-\theta,\tau)$ of nodes $i\in[1,n]$ each given by (29) as [15]

$$\mathsf{M}_{S^{e2e}}\left(-\theta,\tau\right)\leq \mathsf{M}_{S_1^{lo}} * \mathsf{M}_{S_2^{lo}} *\cdots * \mathsf{M}_{S_n^{lo}}\left(-\theta,\tau\right). \quad (32)$$

The multiplexing gain inherent in this formulation lies in the convolution of the MGFs. It uses the independence of the cross traffic at the tandem nodes by multiplication of the MGFs at *every* point in time. An end-to-end delay bound for the through flow $\mathsf{P}\left[W>d\right]\leq\varepsilon^{e2e}$ follows by insertion of (32) into Th. 3 in [15]. The end-to-end delay bound scales linearly in the number of nodes n, i.e., in $\mathcal{O}\left(n\right)$ [15].

B. Convolution Gain in Tandem Networks using Envelopes

End-to-end performance bounds based on envelope functions are derived in [14]. The computation of such bounds relies on a fundamental network service curve representation, which is composed of the individual nodes' statistical service curves. An end-to-end service curve of the through flow in Fig. 7 is obtained by convolution of the leftover service curves $S_i(t)$ of nodes $i\in[1,n]$ each given by (31) with violation probability $\varepsilon_i(b)$ as [14]

$$S^{e2e}(t)=S_1\otimes S_2^{-\delta}\otimes\cdots\otimes S_n^{-(n-1)\delta}(t) \quad (33)$$

where $S_i^{-\delta}(t)=S_i(t)-\delta t$ and $\delta>0$ is a free parameter. The superscript δ denotes a slack rate subducted from the service rate to enable formulating a network service curve. It stems from a sample path description of the departures of the first $(n-1)$ nodes. The violation probability is given by $\varepsilon_i^{\delta}(b)=1/\delta\int_b^{\infty}\varepsilon_i\left(u\right)du$. The network service curve (33) satisfies (30) with violation probability $\varepsilon^{e2e}(b)$ where, *without* assumption of statistical independence, [14]

$$\varepsilon^{e2e}(b)=\varepsilon_1^{\delta}\otimes\cdots\otimes\varepsilon_{n-1}^{\delta}\otimes\varepsilon_n(b). \quad (34)$$

End-to-end performance bounds derived from (33) and (34) for an n node network grow as $\Theta\left(n\log n\right)$ [18], [27].

The formulation of end-to-end service curves (33) and (34) can be adapted to take advantage of statistical independence of the individual nodes [25], Ch. 6. A result on the growth of end-to-end delay bounds with the number nodes that can be obtained from (33) under statistical independence is, however, not provided in [25]. In the sequel, we derive such a result.

Given the end-to-end service curve (33). If the individual nodes, respectively, the cross flows at these nodes are statistically independent, then (33) satisfies the definition of service curve (30) with violation probability [25]

$$\varepsilon^{e2e}(b)=\varepsilon_1^{\delta}*\cdots *\varepsilon_{n-1}^{\delta}*\varepsilon_n(b), \quad (35)$$

i.e., under statistical independence (35) can be used instead of (34) to improve the violation probability. The result is proven as Th. 6.13 in [25]. Here, we only seek to provide the intuition behind the proof, that is (6.21) in [25] p. 129. To this end, we use random variables Y_i that each correspond to a sample path argument for the departures of the ith node, respectively, the arrivals of the $i+1$th node for $i\in[1,n-1]$[1]. In brief, Y_i can be viewed as the maximal difference between the actual (random) departures of a node and the departures as predicted by its service curve subject to the slack rate δ. The random variables Y_i each have the CCDF bound ε_i^{δ} such that a CCDF bound for the sum of all statistically independent Y_i for $i\in[1,n]$ follows as (35). Following Th. 6.4 in [25] pp. 123, end-to-end delay bounds can be derived from (33) and (35).

C. A Scaling Result for End-to-end Performance Bounds

Next, we derive a scaling of performance bounds as obtained under statistical independence from (33) and (35) if the number of nodes n increases. This scaling specifies the price paid in terms of a higher delay bound for longer network paths under the premise of a constant violation probability ε^{e2e}.

Consider the through flow in Fig. 7 that traverses n homogeneous nodes each with capacity C and independent EBB cross traffic. For a fixed violation probability ε^{e2e}, the end-to-end delay and backlog bounds for the through traffic as obtained from (35), and (33) grow with n as

$$\mathcal{O}\big(n\log\left(n\right)\big). \quad (36)$$

The proof of (36) is given in the appendix. The result provided by (36) compares to similar scaling results for EBB, respectively, $(\sigma(\theta),\rho(\theta))$ traffic. In Sect. V-A we reviewed the result of the MGF representation that achieves a scaling of $\mathcal{O}\left(n\right)$ [15] under the same set of assumptions.

[1]The nth node is a minor technical exception since the departures are not arrivals to a subsequent node such that a sample path argument is not required and Y_n is a simple point-wise argument.

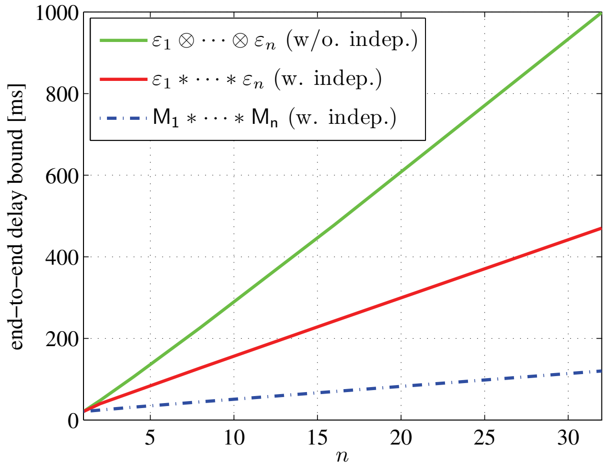

Fig. 8. End-to-end delay bounds as obtained from the different models with, respectively, without assumption of statistical independence. The violation probability ε^{e2e} is fixed to 10^{-9}.

Fig. 8 depicts numerical results for end-to-end delay bounds for the scenario in Fig. 7. We consider, e.g., an MPLS traffic trunk over n nodes with CBR through traffic with mean rate 50 Mbps. The cross traffic is generated by on-off-sources with parameters $P = 60$Mbps, $\lambda = 25$Mbps and $T = 10$ms. All nodes have a capacity $C = 100$Mbps. We fix $\varepsilon^{e2e} = 10^{-9}$ and optimize the free parameters numerically. We observe a numerical improvement of the delay bound if independence of the cross traffic flows is assumed. Notice the difference of the numerical delay bounds for independent cross traffic obtained in Sect. V-A and Sect. V-B, respectively.

In this section we compared scaling results for end-to-end delay bounds under independent EBB cross traffic. We derived a scaling for end-to-end delay bounds using envelope functions based on the framework given in [25] for statistically independent nodes. We showed the fundamental difference in the model formulation and respective scaling results compared to the MGF calculation in Sect. V-A.

VI. Conclusions

In this work we systematically analyzed the impact of statistical multiplexing on the performance of communication networks. We distinguished different independence assumptions that contribute to the multiplexing gain. We compared multiplexing results of different traffic models through the derivation of performance bounds, e.g., on backlog or delay for class EBB traffic. We quantified the advantage of representing traffic superposition using the moment generating function. Further, we evaluated the statistical multiplexing gain using practical examples of network dimensioning that highlight, e.g., the impact of scheduling. In addition, we showed multiplexing gain in multi-node scenarios, i.e., convolution-form networks. We contributed a scaling of end-to-end delay bounds with the number of nodes n for independent EBB cross traffic, that is characterized by envelope functions.

Appendix

A. Lemma 1

Proof: Let X_1, X_2 be two independent random variables with cumulative distribution functions (CDFs) $F_{X_1}(b)$ and $F_{X_2}(b)$. The random variables X_1, X_2 have CCDFs $1 - F_{X_i}(b) = \alpha e^{-\theta b}$ for $b \geq b^* = \frac{1}{\theta}\log\alpha$, where b^* satisfies $F_{X_i}(b^*) = 0$ for $i \in [1,2]$. First, we compute the PDFs $f_{X_i}(b) = \frac{d}{db}(1-\alpha e^{-\theta b}) = \alpha\theta e^{-\theta b}$ for $i \in [1,2]$ and $b \geq b^*$ and zero otherwise. The PDF of the sum $X_1 + X_2$, i.e., $f_{X_1+X_2}(b)$ is given by the convolution

$$\begin{aligned} f_{X_1+X_2}(b) &= \int_{b^*}^{b-b^*} f_{X_1}(a) f_{X_2}(b-a)da \\ &= \int_{b^*}^{b-b^*} \alpha\theta e^{-\theta a}\alpha\theta e^{-\theta(b-a)}da \\ &= \alpha^2\theta^2 e^{-\theta b}(b - 2b^*) \end{aligned}$$

for $b \geq 2b^*$. The CDF of the sum $X_1 + X_2$ is given by

$$\begin{aligned} F_{X_1+X_2}(b) &= \int_{2b^*}^{b} f_{X_1+X_2}(u)du \\ &= \int_{2b^*}^{b} \alpha^2\theta^2 e^{-\theta u}(u - 2b^*)du \\ &= 1 - \alpha^2\left(1 + \theta b - 2\log\alpha\right)e^{-\theta b} \end{aligned}$$

for $b > 2b^*$. We use the integration by parts rule $\int u e^{-\theta u}du = -\frac{(1+\theta u)}{\theta^2}e^{-\theta u}$. The CCDF of the sum $X_1 + X_2$ is given by

$$1 - F_{X_1+X_2}(b) = \alpha^2\left(1 + \theta b - 2\log\alpha\right)e^{-\theta b}. \qquad (37)$$

For the second part of Lem. 1 we regard two pairs of independent random variables $\{Z_1, Z_2\}$ and $\{X_1, X_2\}$ with following stochastic ordering $X_i \geq_{st} Z_i$ for $i \in [1,2]$. The shorthand notation $X_i \geq_{st} Z_i$ is defined in terms of the CCDFs as

$$1 - F_{X_i}(b) \geq 1 - F_{Z_i}(b)$$

for $b \geq 0$, where $F_{X_i}(b)$ and $F_{Z_i}(b)$ are the CDFs of X_i and Z_i, respectively. Under the above assumptions it holds that $X_1 + X_2 \geq_{st} Z_1 + Z_2$, see [28] such that

$$1 - F_{X_1+X_2}(b) \geq 1 - F_{Z_1+Z_2}(b).$$

for $b \geq 0$. By insertion of $1 - F_{X_i}(b) = \alpha e^{-\theta b}$ for $b \geq b^* = \frac{1}{\theta}\log\alpha$ it follows with (37) for the sum of two independent random variables Z_1 and Z_2 with $1 - F_{Z_i}(b) \leq \alpha e^{-\theta b}$ that $1 - F_{Z_1+Z_2}(b) \leq \alpha^2\left(1 + \theta b - 2\log\alpha\right)e^{-\theta b}$. ■

B. Lemma 2

Proof: We seek to bound the linear function $g(b) = (1 + \theta b - 2\log\alpha)\alpha^2$ for all b from above using an expression of the form $h(b) = Ke^{\phi b}$ with free parameter $\phi > 0$. In the following, we calculate K such that $g(b) \leq h(b)$ is satisfied for all b, for any given choice of $\phi > 0$.

We equate $\frac{\partial}{\partial b}g(b) = \frac{\partial}{\partial b}h(b)$ and solve for $b = \frac{1}{\phi}\log\frac{\theta\alpha^2}{\phi K} := b'$. In the next step we insert b' into $g(b') = h(b')$ and solve for K, where K is given in Lem. 2. Since $\frac{\partial^2}{\partial b^2}g(b) = 0$ and $\frac{\partial^2}{\partial b^2}h(b) > 0$ for all b it holds that $g(b) \leq h(b)$ for all b.

Finally, to ensure that $Ke^{-(\theta-\phi)b}$ in Lem. 2 is decreasing in b, we restrict ϕ to $(0, \theta)$. ■

C. Derivation of (23)

Consider the superposition of two homogeneous flows, where each flow has the envelope (22). We invoke Lem. 1 with $\alpha = e^{\theta\sigma(\theta)}e^{-\theta\beta(\theta)\tau}$ to compute the violation probability of the sum

$$\begin{aligned} &\mathsf{P}\left[(A_1+A_2)(t,t+\tau)-(E_1+E_2)(\tau)>b\right] \\ &\quad\leq \left(1+\theta b-2\theta\sigma\left(\theta\right)+2\theta\beta(\theta)\tau\right)e^{2\theta\sigma(\theta)}e^{-2\theta\beta(\theta)\tau}e^{-\theta b} \end{aligned} \tag{38}$$

for $b \geq 2b^*$ and $b^* = \sigma(\theta) - \beta(\theta)\tau$.

Next, we calculate the sample path violation probability $\varepsilon^s(b)$. The derivation is similar to (14). We apply the union bound and upper bound the sum $\sum_{\tau=1}^{\infty}(\cdot)$ by the integral $\int_0^{\infty}(\cdot)d\tau$ to find $\varepsilon^s(b)$ for the multiplexed flows. Thus, we evaluate the integral

$$e^{2\theta\sigma(\theta)}e^{-\theta b}\int_0^{\infty} e^{-2\theta\beta(\theta)\tau}\left(1+\theta b-2\theta\sigma\left(\theta\right)+2\theta\beta(\theta)\tau\right)d\tau.$$

The evaluation of the four summands of the integral yields

$$\frac{1}{2\theta\beta(\theta)}+\frac{\theta b}{2\theta\beta(\theta)}-\frac{2\theta\sigma(\theta)}{2\theta\beta(\theta)}+\frac{1}{2\theta\beta(\theta)}.$$

For the evaluation of the fourth summand we used integration by parts and the rule of L'Hôpital. After some reordering we obtain the following bound

$$\begin{aligned} &\mathsf{P}\left[(A_1+A_2)\oslash(E_1+E_2)(t)>b\right] \\ &\qquad\leq \left(2+\theta\left(b-2\sigma\left(\theta\right)\right)\right)\frac{e^{2\theta\sigma(\theta)}e^{-\theta b}}{2\theta\beta(\theta)} = \varepsilon^s(b). \end{aligned}$$

D. Derivation of (24)

Consider the superposition of two homogeneous traffic flows characterized each by a sample path envelope (14) with violation probability $\varepsilon_i^s(b) = \frac{e^{\theta\sigma(\theta)}e^{-\theta b}}{\theta\beta(\theta)}$ for $i \in [1,2]$. We resort to Lem. 1 to compute the violation probability of the sum. We insert $\varepsilon_i^s(b)$ into Lem. 1 where we let $\alpha = \frac{e^{\theta\sigma(\theta)}}{\theta\beta(\theta)}$ to derive

$$\begin{aligned} &\mathsf{P}\left[(A_1\oslash E_1)+(A_2\oslash E_2))(t)>b\right] \\ &\quad\leq \left(1+\theta b-2\log\left(\frac{e^{\theta\sigma(\theta)}}{\theta\beta(\theta)}\right)\right)\left(\frac{e^{\theta\sigma(\theta)}}{\theta\beta(\theta)}\right)^2 e^{-\theta b} \end{aligned}$$

for $b \geq 2b^*$ and $b^* = \frac{1}{\theta}\log\left(\frac{e^{\theta\sigma(\theta)}}{\theta\beta(\theta)}\right)$. After some reordering (24) is obtained.

E. Derivation of (25)

The following lemma provides an EBB type bound on the result of the convolution of $N = 2^k$ violation probabilities, $k \in \mathbb{N}$. The result is obtained through successive insertion in Lem. 1 and Lem. 2 until the desired N is achieved. This recursion can be illustrated as a dyadic scheme.

Lemma 3 (EBB type bound for multiplexed EBB flows)**.** *Under the assumptions of Lem. 1 and Lem. 2. For $N = 2^k$ violation probabilities $\varepsilon_i(b) \leq \alpha e^{-\theta b}$ for $i \in [1,N]$, $k \in \mathbb{N}$, it holds that*

$$\varepsilon_1 * \cdots * \varepsilon_N(b) \leq H_k \cdot \alpha^{\frac{N(\theta-k\phi)}{\theta}} \cdot e^{-(\theta-k\phi)b}$$

where $\phi \in (0,\theta/k)$ is a free parameter and

$$H_k = \prod_{i=1}^{k}\left(\frac{\theta-(k-i)\,\phi}{\phi}\right)^{2^{i-1}\frac{\theta-k\phi}{\theta-(k-i+1)\phi}} e^{-\frac{z_k}{\prod_{i=1}^{k}(\theta-(i-1)\phi)}}.$$

with $z_k = (2z_{k-1}+\prod_{i=1}^{k-1}\left(\theta-(i-1)\,\phi\right))\left(\theta-k\phi\right)$ for $k>1$ and $z_1 = \theta-\phi$.

We proved Lem. 3 by induction. The k-fold alternating insertion into Lem. 1 and Lem. 2 leads to degrading the exponent of the EBB type bound by $k\phi$.

For derivation of (25) we consider the superposition of $N = 2^k$ independent traffic flows, $k \in \mathbb{N}$, each characterized by (22). We substitute into Lem. 3 with $\alpha = e^{\theta\sigma(\theta)}e^{-\theta\beta(\theta)\tau}$ to find the following EBB type bound on the violation probability

$$\begin{aligned} &\mathsf{P}\left[\sum_{i=1}^{N}A_i(t,t+\tau)-\sum_{i=1}^{N}E_i(\tau)>b\right] \\ &\qquad\qquad\leq H_k e^{-N(\theta-k\phi)(\beta(\theta)\tau-\sigma(\theta))}e^{-(\theta-k\phi)b}, \end{aligned}$$

where $\theta > 0$ and $\phi \in (0,\theta/k)$ are free parameters and H_k is given in Lem. 3.

Next, we calculate the sample path violation probability along the same line as (14). We invoke the union bound and upper bound the sum $\sum_{\tau=1}^{\infty}(\cdot)$ by the integral $\int_0^{\infty}(\cdot)d\tau$ to obtain the sample path violation probability. Thus, we evaluate the integral $\int_0^{\infty}H_k e^{-N(\theta-k\phi)(\beta(\theta)\tau-\sigma(\theta))}e^{-(\theta-k\phi)b}d\tau$ to find

$$\mathsf{P}\left[\left(\textstyle\sum_i A_i\right)\oslash\left(\textstyle\sum_i E_i\right)(t)>b\right] \leq H_k\frac{e^{N(\theta-k\phi)\sigma(\theta)}}{(\theta-k\phi)N\beta(\theta)}e^{-(\theta-k\phi)b}.$$

F. Derivation of (26)

The derivation resorts to Lem 3. We superpose N independent traffic flows each characterized by sample path envelopes, i.e., traffic model B2. The superposition implies convolving the respective sample path violation probabilities. To this end, we calculate for each flow $i \in [1,N]$ the sample path violation probability $\varepsilon_i^s(b)$ derived as in (14), i.e., $\varepsilon_i^s(b) = \frac{e^{\theta\sigma(\theta)}e^{-\theta b}}{\theta\beta(\theta)}$.

We substitute into Lem 3 with $\alpha = \frac{e^{\theta\sigma(\theta)}}{\theta\beta(\theta)}$ to find the following sample path violation probability for $N = 2^k$ with $k \in \mathbb{N}$

$$\mathsf{P}\left[\textstyle\sum_i(A_i\oslash E_i)(t)>b\right] \leq H_k\cdot\left(\frac{e^{\theta\sigma(\theta)}}{\theta\beta(\theta)}\right)^{N\frac{\theta-k\phi}{\phi}} e^{-(\theta-k\phi)b}$$

with free parameters $\theta > 0$ and $\phi \in (0,\theta/k)$. H_k is given in Lem. 3.

G. Proof of (36)

We regard an n node tandem network with CBR through traffic and EBB cross traffic with sample path envelope $E^{cr}(\tau) = (\rho^{cr}+\beta^{cr})\tau$ at each node $i \in [1,n]$. An end-to-end service curve is obtained from (33)[2] as $S^{e2e}(\tau) = (C-(\rho^{cr}+\beta^{cr})-n\delta)\tau$ with free parameter $\delta > 0$. Next, we calculate the end-to-end violation probability $\varepsilon^{e2e}(b)$. Under statistical independence, $\varepsilon^{e2e}(b)$ is given in (35)[3] by convolution of

[2]For ease of exposition we estimate $(n-1)\delta$ by $n\delta$.

[3]Again for ease of exposition, we neglect the irregularity of the last term and substitute $\varepsilon_n^{\delta}(b)$ for $\varepsilon_n(b)$.

violation probabilities $\varepsilon_i^{\delta}(b)$ for $i \in [1,n]$. We derive $\varepsilon_i^{\delta}(b)$ for node $i \in [1,n]$ from $\varepsilon^s(b)$ given in (14) as

$$\varepsilon_i^{\delta}(b) = \frac{1}{\delta}\int_b^{\infty} \frac{e^{\theta\sigma(\theta)}e^{-\theta u}}{\theta\beta(\theta)}du = \frac{e^{\theta\sigma(\theta)}e^{-\theta b}}{\delta\theta^2\beta(\theta)} := Ge^{-\theta b}$$

with free parameters $\theta > 0$, $\beta(\theta) > 0$, and $\delta > 0$.

To calculate $\varepsilon^{e2e}(b)$ we combine the violation probabilities ε_i^{δ} for $i \in [1,n]$ nodes using Lem. 3. For $n = 2^k$ nodes, $k \in \mathbb{N}$ to find

$$\varepsilon^{e2e}(b) \leq H_k \cdot G^{n\frac{\theta - k\phi}{\theta}} \cdot e^{-(\theta - k\phi)b} \tag{39}$$

where $\theta > 0$ and $\phi \in (0, \theta/k)$ are free parameters and H_k is given in Lem. 3. We upper bound the prefactor in (39) such as

$$\varepsilon^{e2e}(b) \leq \left(\frac{\theta G}{\phi}\right)^n e^{-(\theta-k\phi)b} = \left(\frac{ne^{\theta\sigma(\theta)}}{\phi\Delta\theta\beta(\theta)}\right)^n e^{-(\theta-k\phi)b} \tag{40}$$

where we use a constant $\Delta > 0$ and let $\delta = \Delta/n$ to keep the network service curve fixed for different n. Next, we derive the growth of b in (40) for constant violation probability ε^{e2e}. We set the free parameter $\phi = c_0/k$ using a positive constant c_0 and use positive constants c_1 and c_2 to substitute all terms that do not depend on b, n or ε^{e2e} such that we can solve (40) for b as

$$\varepsilon^{e2e} \leq (c_1 n \log_2(n))^n e^{-c_2 b}$$
$$\Rightarrow b \leq 1/c_2 \left(n \log\left(c_1 n \log_2(n)\right) - \log\left(\varepsilon^{e2e}\right)\right).$$

This implies that b grows as $\mathcal{O}(n\log(n))$ to meet the constraint of constant ε^{e2e} for all n. Note that $\phi = c_0/k$, is the function of the highest order that satisfies the constraint $\phi < \theta/k$ for all n. An alternative proof of (36) using MGFs can be found in [1].

REFERENCES

[1] A. Rizk and M. Fidler, "Leveraging multiplexing gains in single- and multi-hop networks," in *Proc. 2011 IEEE/ACM IWQoS*.

[2] L. Kleinrock, "Message delay in communication nets with storage," Ph.D. dissertation, MIT, Dec. 1962.

[3] J. Liebeherr, S. Patek, and E. Yilmaz, "Tradeoffs in designing networks with end-to-end statistical QoS guarantees," in *Proc. 2000 IEEE/ACM IWQoS*, pp. 221–230.

[4] A. Elwalid, D. Mitra, and R. H. Wentworth, "A new approach for allocating buffers and bandwidth to heterogeneous, regulated traffic in an ATM node," *IEEE J. Sel. Areas Commun.*, vol. 13, pp. 1115–1127, 1995.

[5] F. P. Kelly, "Notes on effective bandwidths," ser. Royal Statistical Society Lecture Notes. Oxford University Press, 1996, no. 4, pp. 141–168.

[6] J. Choe and N. B. Shroff, "A central-limit-theorem-based approach for analyzing queue behavior in high-speed networks," *IEEE/ACM Trans. Netw.*, vol. 6, no. 5, pp. 659–671, 1998.

[7] E. W. Knightly and N. B. Shroff, "Admission control for statistical QoS: theory and practice," *IEEE Network*, vol. 13, no. 2, pp. 20–29, 1999.

[8] R. R. Boorstyn, A. Burchard, J. Liebeherr, and C. Oottamakorn, "Statistical service assurances for traffic scheduling algorithms," *IEEE J. Sel. Areas Commun.*, vol. 18, no. 12, pp. 2651–2664, Dec. 2000.

[9] R. Mazumdar, *Performance Modeling, Loss Networks, and Statistical Multiplexing*. Morgan & Claypool Publishers, 2010.

[10] O. Yaron and M. Sidi, "Performance and stability of communication networks via robust exponential bounds," *IEEE/ACM Trans. Netw.*, vol. 1, no. 3, pp. 372–385, June 1993.

[11] R. L. Cruz, "Quality of service management in integrated services networks," in *Proc. 1996 Research Review*.

[12] C. S. Chang, "Stability, queue length, and delay of deterministic and stochastic queueing networks," *IEEE Trans. Automat. Contr.*, vol. 39, no. 5, pp. 913–931, May 1994.

[13] Q. Yin, Y. Jiang, S. Jiang, and P. Y. Kong, "Analysis of generalized stochastically bounded bursty traffic for communication networks," in *Proc. 2002 IEEE LCN*, pp. 141–149.

[14] F. Ciucu, A. Burchard, and J. Liebeherr, "Scaling properties of statistical end-to-end bounds in the network calculus," *IEEE Trans. Inf. Theory*, vol. 14, no. SI, pp. 2300–2312, June 2006.

[15] M. Fidler, "An end-to-end probabilistic network calculus with moment generating functions," in *Proc. 2006 IWQoS*, pp. 261–270.

[16] Y. Jiang, "A basic stochastic network calculus," in *Proc. 2006 ACM SIGCOMM*, pp. 123–134.

[17] F. Ciucu, J. Schmitt, and H. Wang, "On expressing networks with flow transformations in convolution-form," in *Proc. 2011 IEEE INFOCOM*, pp. 1979–1987.

[18] F. Ciucu, "Scaling properties in the stochastic network calculus," Ph.D. dissertation, Univ. of Virginia, Aug. 2007.

[19] M. Fidler, "A survey of deterministic and stochastic service curve models in the network calculus," *IEEE Commun. Surveys and Tutorials*, vol. 12, no. 1, pp. 59–86, 2010.

[20] R. L. Cruz, "A calculus for network delay, part I and II: network elements in isolation and network analysis," *IEEE Trans. Inf. Theory*, vol. 37, no. 1, pp. 114–141, Jan. 1991.

[21] ——, "Quality of service guarantees in virtual circuit switched networks," *IEEE J. Sel. Areas Commun.*, vol. 13, no. 6, pp. 1048–1056, Aug. 1995.

[22] C. Li, A. Burchard, and J. Liebeherr, "A network calculus with effective bandwidth," *IEEE/ACM Trans. Netw.*, vol. 15, no. 6, pp. 1442–1453, Dec. 2007.

[23] C. S. Chang, *Performance Guarantees in Communication Networks*. Springer, 2000.

[24] G. Grimmett and D. Stirzaker, *Probability and Random Proceesses*. Oxford University Press, 2001.

[25] Y. Jiang and Y. Liu, *Stochastic Network Calculus*. Springer, 2008.

[26] L. Breslau, D. Estrin, K. Fall, S. Floyd, J. Heidemann, A. Helmy, P. Huang, S. McCanne, K. Varadhan, Y. Xu, and H. Yu, "Advances in network simulation," *Computer*, vol. 33, no. 5, pp. 59–67, 2000.

[27] A. Burchard, J. Liebeherr, and F. Ciucu, "On $\Theta(H \log H)$ scaling of network delays," in *Proc. 2007 IEEE INFOCOM*, pp. 1866–1874.

[28] D. Stoyan, *Comparison Methods for Queues and Other Stochastic Models*. John Wiley & Sons, 1983.

Amr Rizk graduated in electrical engineering and business administration from the Technische Universität Darmstadt in 2008. Since May 2008, he has been working towards the Ph.D. degree in electrical and computer engineering at the Institute for Communications Technology at the Leibniz Universität Hannover. He is a member of the Emmy Noether Research Group "ProPerBounds" funded by the German Research Foundation (DFG).

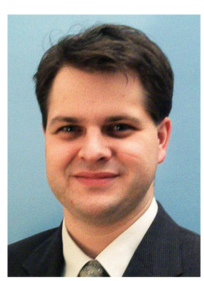

Markus Fidler (M04–SM08) received the doctoral degree in computer engineering from RWTH Aachen University, Germany, in 2004. He was a Post-Doctoral Fellow of NTNU Trondheim, Norway, in 2005 and the University of Toronto, ON, Canada, in 2006. During 2007 and 2008, he was an Emmy Noether Research Group Leader at Technische Universität Darmstadt, Germany. Since 2009, he has been a Professor of communications networks at Leibniz Universität Hannover, Germany.